# Performance Analysis of Phase-Coded FMCW for Joint Sensing and Communication

Kumbul, Utku; Petrov, Nikita; Vaucher, Cicero S.; Yarovoy, Alexander

**DOI**
10.23919/IRS57608.2023.10172426

**Publication date**
2023

**Document Version**
Final published version

**Published in**
2023 24th International Radar Symposium, IRS 2023

**Citation (APA)**
Kumbul, U., Petrov, N., Vaucher, C. S., & Yarovoy, A. (2023). Performance Analysis of Phase-Coded FMCW for Joint Sensing and Communication. In *2023 24th International Radar Symposium, IRS 2023* (Proceedings International Radar Symposium; Vol. 2023-May). IEEE. https://doi.org/10.23919/IRS57608.2023.10172426

# Performance Analysis of Phase-Coded FMCW for Joint Sensing and Communication

**Utku Kumbul***, **Nikita Petrov****, **Cicero S. Vaucher****, **Alexander Yarovoy***

*Department of Microelectronics, Delft University of Technology,
Delft, THE NETHERLANDS
email: u.kumbul@tudelft.nl

**NXP Semiconductors
Eindhoven, THE NETHERLANDS
email: cicero.vaucher@nxp.com

***Abstract:*** *Phase-coded frequency modulated continuous wave (PC-FMCW) radars for joint sensing and communication are considered. The sensing and communication performance of the two signal processing methods, phase lag compensated group delay filter and filter bank receivers, are compared. It is demonstrated that the phase lag compensated group delay receiver provides better sensing performance and requires less computational complexity than the filter bank receiver. The application of the former receiver is, however, limited by the bit error rate degradation with the communication signal bandwidth.*

## 1. Introduction

Autonomous driving has become a new emerging technology that will improve road safety. Traditional autonomous driving systems utilize wireless sensors for vehicle-to-vehicle (V2V) communication and radar sensors for providing self-awareness about the environment. Sharing a limited radio frequency spectrum by numerous wireless devices raises a concern about spectral congestion [1, 2]. Therefore, there is a growing interest towards joint sensing and communication systems to combine the functionalities of both of these sensors and reduce the spectrum crowding [3, 4, 5]. To enable joint radar-communication (RadCom) coexistence, various methods and waveform design techniques are studied [6, 7, 8]. Since the automotive radars rely on simple hardware and low processing power, cost-efficient methods to realize RadCom systems are still of interest.

One promising approach to achieve the aforementioned task is using a communication signal to modulate the chirp signal. To this end, phase-coded frequency modulated continuous wave (PC-FMCW) radars have been studied [9, 10, 11]. In the PC-FMCW radar, the phase-coded signals are used to modulate the phase changes within the chirp. The key advantage of PC-FMCW waveforms lies in the ability to use dechirping-based receivers to reduce the waveform sampling requirements. Thus, the PC-FMCW waveforms can carry information while maintaining the benefits of frequency modulated continuous wave (FMCW) signal, such as good Doppler


978-3-944976-34-1 ©2022 DGON

tolerance, high range resolution and low sampling requirement [12, 13, 14, 15]. These make the utilization of PC-FMCW waveforms suitable for automotive radars.

For the dechirping based receivers, the compensated stretch processing and the group delay filter receivers are proposed in [14, 15]. The compensated stretch processing performs a matched filter to the dechirped signals via a filter bank for all ranges of interest. Such an operation raises the computational complexity compared to conventional stretch processing. On the other hand, the group delay filter receiver aligns the dechirped signals and then decodes with the reference phase-coded signal to obtain a beat signal. After decoding, range information can be extracted similarly to standard chirp processing by performing a fast Fourier transform (FFT). However, the group delay filter leads to an unwanted quadratic phase shift, which distorts the received code inside the dechirped signal. As a consequence, the range sidelobe levels increases, especially for a code with large bandwidth due to imperfection in decoding [16]. This undesired effect of the group delay filter receiver is addressed by performing phase lag compensation to the transmitted phase-coded signal before transmission [17]. However, the impact of phase lag compensated group delay filter on the recovery of communication data and the communication performance of such a receiver have not been investigated yet.

In this paper, we investigate both the communication and sensing performance of two receiver strategies for the PC-FMCW waveform: the phase lag compensated group delay filter and filter bank approaches. To accomplish this goal, we give the signal model for two signal processing methods in Section 2. Subsequently, we examine the two aforementioned approaches to reconstruct the communication data from the received signal in Section 3. Then in Section 4, the sensing and communication performance comparison of the two methods are presented. Finally, we draw the conclusions in Section 5.

## 2. Signal Processing for Sensing

Assume a phase-coded signal $s(t)$ is used to modulate phase changes inside the chirp signal with a chirp duration $T$ and chirp bandwidth $B$. In the PC-FMCW radar, $N_c$ number of chips per chirp is used for fast-time coding, and the chip duration becomes $T_c = T/N_c$. Consequently, the code bandwidth is controlled by the number of chips inside the chirp as $B_c = N_c/T$. Herein, we assume the code bandwidth is much smaller than the chirp bandwidth to avoid spectrum leakage. Then, the transmitted PC-FMCW waveform can be written as:

$$x_{\mathrm{t}}(t) = s(t)e^{-j(2\pi f_c t + \pi k t^2)}, \ \ t \in [0, T], \tag{1}$$

where $k = B/T$ is the chirp slope and $f_c$ is the carrier frequency. The transmitted signal (1) is reflected from a target with constant velocity and received with a round trip delay as:

$$x_{\mathrm{r}}(t) = \alpha_0 s(t - \tau(t))e^{-j(2\pi f_c (t-\tau(t)) + \pi k (t-\tau(t))^2)}, \tag{2}$$

where $\tau(t)$ is the round-trip delay, and $\alpha_0$ is a complex amplitude proportional to a target backscattering and propagation effects. The round trip delay can be represented as:

$$\tau(t) = \frac{2\left(R_0 + v_0\,(t)\right)}{c} = \tau_0 + \frac{2v_0}{c}\,(t)\,, \tag{3}$$

where $c$ is the speed of light, $R_0$ is the range, and $v_0$ is the velocity. During the dechirping process, the received signal is mixed with the complex conjugate of the uncoded chirp signal. Then, the dechirped signal can be written as [16]:

$$\begin{aligned} x_{\mathrm{b}}(t) &= x_{\mathrm{r}}(t) e^{j\left(2\pi f_c t + \pi k t^2\right)} \\ &= \alpha_0 s\left(t - \tau(t)\right) e^{j\left(2\pi f_c \tau_0 + 2\pi(k\tau_0 + f_d)t - \pi k {\tau_0}^2\right)} \\ &\approx \alpha_0 s(t-\tau_0) e^{j(2\pi f_b t)}, \end{aligned} \tag{4}$$

where $f_b = k\tau_0 + f_d \approx k\tau_0$ is the beat frequency. Herein, $f_d = 2v_0 f_c/c$ is the Doppler frequency shift in the fast-time, and it can be neglected during fast-time processing since it is typically much smaller than the one range cell, $f_d \ll f_s/N$, where $f_s$ is the sampling frequency of the beat signal and $N$ is the number of fast-time samples. Moreover, we incorporate all the constant terms of signal processing into $\alpha_0$ without loss of generality. The dechirped signal has two main components, the delayed phase-coded signal and the beat signal. In the following subsections, we will examine two processing methods to reconstruct the range profile.

### 2.1. Filter bank receiver

The filter bank receiver applies a matched filter to a sampled dechirped signal for all ranges of interest. Such a method is called compensated stretch processing in [14]. In the filter bank receiver, a reference phase-coded signal is shifted for each range hypothesis defined by $\tau$, and the receiver performs [16]:

$$y(\tau) = \int_0^T x_{\mathrm{b}}(t) s^*\left(t-\tau\right) e^{-j(2\pi k\tau t)} dt, \tag{5}$$

where $(\cdot)^*$ denotes the complex conjugate. To perform this integral, the dechirped signal (4) is sampled by analog-to-digital convertor (ADC) with the sampling frequency $f_s$ and stored in a vector as:

$$\mathbf{x}_{\mathrm{b}} = \alpha_0 s\left(n/f_s - \tau_0\right) e^{j(2\pi k\tau_0 n/f_s)}, \tag{6}$$

where $\mathbf{x}_{\mathrm{b}} \in \mathbb{C}^{N\times 1}$ and $t = n/f_s, n = 0, \ldots, N-1$. For each given $\tau$, the hypothesis part in the integral (5) can be written via a Hadamard product of two vectors $\mathbf{b}(\tau) \odot \mathbf{s}(\tau)$:

$$\begin{aligned} \mathbf{b}(\tau) &= e^{j(2\pi k\tau n/f_s)}, \\ \mathbf{s}(\tau) &= s\left(n/f_s - \tau\right), \end{aligned} \tag{7}$$

where $\mathbf{b}(\tau), \mathbf{s}(\tau) \in \mathbb{C}^{N\times 1}, n = 0, \ldots, N-1$. Then, the vectors with different $\tau$ are stacked up in columns and stored in the $N \times N_r$ matrices as $\mathbf{B} = [\mathbf{b}(\tau_0), \ldots, \mathbf{b}(\tau_{N_r})]$ and $\mathbf{S} = [\mathbf{s}(\tau_0), \ldots, \mathbf{s}(\tau_{N_r})]$, where the number of range cells in the range grid denoted by $N_r$. Subsequently, the convolution (5) can be represented via a matrix-vector product as [16]:

$$\mathbf{y} = \left(\mathbf{B} \odot \mathbf{S}\right)^H \mathbf{x}_{\mathrm{b}} \tag{8}$$

The resulting vector $\mathbf{y}$ contains the range profile. It is important to note that applying the filter bank receiver requires a matrix multiplication and leads to the computational complexity of Discrete Fourier Transform (DFT) $\mathcal{O}(N^2)$.

### 2.2. Phase Lag Compensated Group Delay Filter Receiver

The group delay filter receiver aims to decode the communication signal first and then perform FFT to the resulting beat signal for range processing. For this purpose, this receiver applies a group delay filter for the alignment of all coded beat signals in the fast-time before decoding with the reference code signal [15]. However, such a filter causes a dispersion effect on the received code, which degrades the sensing performance [16]. To eliminate this unwanted effect, the phase lag compensation (PLC) is performed on the transmitted phase-coded signal before transmission. Such a PLC filter can be written as [17]:

$$H_{\text{lag}}(f) = e^{-j\left(\frac{\pi f^2}{k}\right)}, \tag{9}$$

The spectrum of the transmitted code is multiplied by the resulting PLC filter before transmission. Then the dechirped signal given in (4) can be recast as:

$$x_{\text{b}}(t) = \alpha_0 \hat{s}(t-\tau_0)e^{j(2\pi f_b t)}, \tag{10}$$

where $(\hat{\cdot})$ denotes the phase-coded signal that is modified after performing a PLC filter. Afterwards, the group delay filter will be applied to align all coded beat signals. The desired group delay filter should eliminate $\tau_0$ term inside the code, and thus the required group delay can be written as:

$$\tau_{\text{g}}(f)\Big|_{f=f_b} = -\frac{1}{2\pi}\frac{d\theta(f)}{df}\Bigg|_{f=f_b} = -\tau_0 = -f_b/k. \tag{11}$$

Then, the required group delay filter can be given as [17]:

$$H_{\text{g}}(f) = e^{j\left(\frac{\pi f^2}{k}\right)}, \tag{12}$$

Then, the group delay filter (12) is applied to the spectrum of (10) and the resulting signal in the time domain becomes [17]:

$$y_{\text{o}}(t) = \alpha_0 s(t)e^{j(2\pi f_b t)}. \tag{13}$$

As a result, the delay term $\tau_0$ is eliminated, and each coded beat signal is perfectly aligned. Subsequently, the decoding can be performed by multiplying with the complex conjugate of reference code, and the decoded signal can be obtained as [17]:

$$y_{\text{d}}(t) = y_{\text{o}}(t)s^*(t) = \alpha_0 e^{j(2\pi f_b t)}. \tag{14}$$

The range profile can be obtained by performing FFT on the decoded signal. Consequently, this receiver has the computational complexity of FFT $\mathcal{O}(N\log_2(N))$. Moreover, it is important to note that this receiver recovers the beat signal properly, and thus it can re-utilize techniques previously developed for the FMCW radar, such as windowing functions to decrease sidelobe levels.

## 3. Recovery of Communication Signal

For communication purposes, the PC-FMCW waveforms must be synchronized to compensate the delay between the transmitted and received signals. Such synchronization can be achieved using global positioning system (GPS), and synchronized chirp can be generated to minimize the delay between transmitting and receiving channels [10]. Alternatively, the time, frequency and phase offset can be estimated in a data-driven fashion by transmitting initial (pivot) radar-only sweep during predetermined time intervals, and the beat frequency signal can be compensated from the communication signal [14]. Identifying the most effective ways for PC-FMCW waveforms synchronization is an ongoing research topic. In this study, we assume the communication receiver knows the delay of the transmitted waveform and uses the synchronized chirp signal as the reference signal for compensating the beat frequency signal. Then, the received signal (2) captured along with the noise is mixed with the complex conjugate of the reference signal and low-pass filtered to get rid of the chirp signal. Then, the received communication signal with delay can be obtained as:

$$\begin{aligned} x_{\mathrm{s}}(t) =& \{x_{\mathrm{r}}(t) + n(t)\}\, e^{j(2\pi f_c(t-\tau(t))+\pi k(t-\tau(t))^2)} \\ =& \alpha_0 s(t-\tau_0) + \bar{n}(t), \end{aligned} \tag{15}$$

where $n(t)$ is a white complex Gaussian noise signal with power spectral density $N_0$, and $\bar{n}(t)$ is the resulting white complex Gaussian noise signal after dechipring and filtering. Herein, the signal-to-noise ratio (SNR) can be defined as SNR $= {\alpha_0}^2/N_0$. After the mixer, the beat frequency signal will have either zero carrier frequency or a very small frequency offset for the mutually moving transmitter and receiver. Given the knowledge of the delay and waveform parameters, the communication receiver can compensate the delay offset in the code $s(t)$. After delay compensation, the received communication signal can be written as:

$$x_{\mathrm{c}}(t) = \alpha_0 s(t) + \bar{n}(t), \tag{16}$$

Subsequently, the transmitted communication data can be constructed by using techniques such as the Viterbi algorithm, which is widely used for optimal maximum likelihood sequence detection [18]. Note that the filter bank approach will obtain the noisy communication signal given in (16). On the other hand, the phase lag compensated group delay receiver will have the noisy received signal where the communication signal is modified with a PLC filter as $x_{\mathrm{c}}(t) = \alpha_0 \hat{s}(t) + \bar{n}(t)$. In this case, the spectrum of the received communication signal needs to be multiplied with the group delay filter (12) to compensate the effect on a code term initiated by a PLC filter. However, this will distort (lose) some parts of the communication signal due to applying a non-linear shift. The impact of such a distortion on communication performance will be investigated in the following section.

## 4. Performance Assessment

This section assesses the sensing and communication performance of two signal processing approaches. Consider an automotive radar transmits the PC-FMCW waveform at a carrier frequency $f_c = 77$ GHz with chirp duration $T = 25.6$ $\mu$s and chirp bandwidth $B = 300$ MHz.

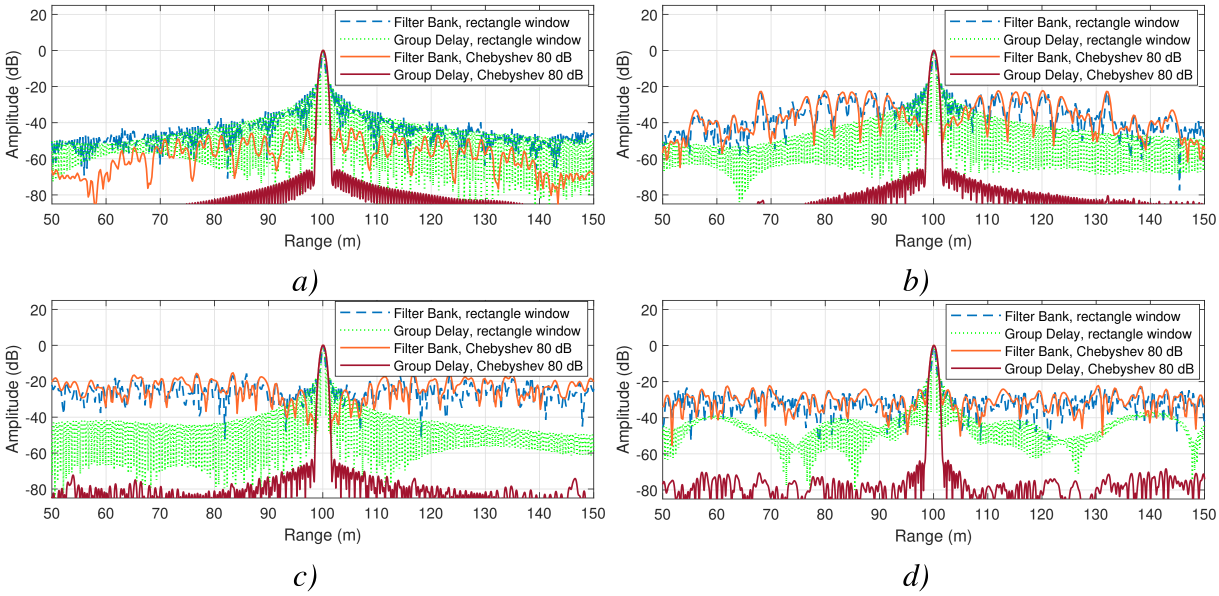


Figure 1: Sensing performance comparison: Range profiles with and without windowing a) $N_c = 16$ b) $N_c = 64$ c) $N_c = 256$ d) $N_c = 1024$

In this study, we consider Gaussian Minimum Shift Keying (GMSK) for the phase modulation of communication signal $s(t)$ as it can provide low spectral broadening [17]. We utilize the random code sequences and set the time-bandwidth product of GMSK coding to $0.3$. The code bandwidth is controlled with the number of chips per chirp as $B_c = N_c/T$, e.g., the code with $N_c = 1024$ number of chips within a sweep has $B_c = 40$ MHz code bandwidth. For the PLC group delay receiver, we perform phase lag compensation before transmission for the GMSK phase-coded signal.

### 4.1. Sensing Performance

In this section, we assume a noise-free scenario to focus on the sensing performance of two processing methods. We consider the transmitted signal reflected from a target at the range $R_0 = 100$ m with a radial velocity $v_0 = 10$ m/s. The received signal is dechirped with the uncoded chirp signal. Then, the dechirped signal (4) is low-pass filtered with the cut-off frequency $f_{cut} = \pm 40$ MHz and sampled through ADC with a sampling frequency $f_s = 80$ MHz. As a result, we have $N = 2048$ range cells (fast-time samples) for the selected system parameters. To prevent signal mismatch, we apply the same LPF to the reference communication signal used for decoding in both receivers. In addition, we normalized the range profiles by the maximum target response to highlight the dynamic range. First, we compare the range profiles of two signal processing approaches. The investigated receivers perform different techniques for range processing, as explained in Section 2. In the PLC group delay filter receiver, the group delay filter is applied to the sampled signal to align the beat signals of different targets. Subsequently, the code term is removed after decoding, and the beat signal is recovered similar to the dechirped signal of traditional FMCW. Thus, this receiver can properly utilize windowing functions to further suppress the sidelobe levels. To highlight the advantages of the PLC group delay

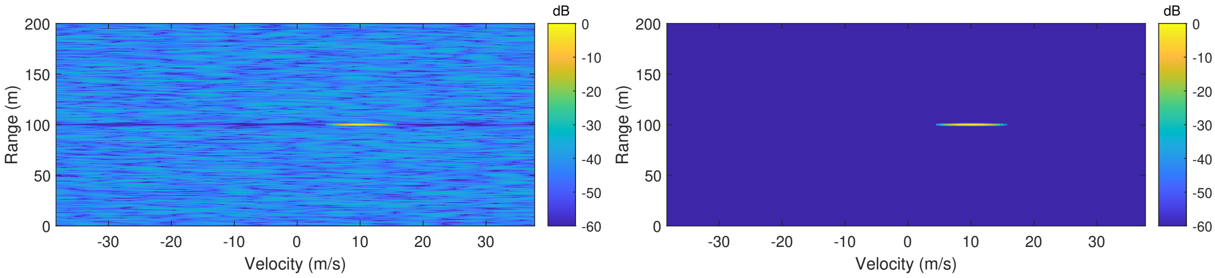


Figure 2: Range-Doppler profile comparison with windowing ($N_p = 32$ and $N_c = 1024$): a) Filter bank receiver b) PLC group delay filter receiver

receiver, we apply $80$ dB Chebyshev window for both receiver methods before range processing and compare it with a rectangle windowing case in Fig. 1. It can be seen that the filter bank approach has a noise-like response outside of the main beam, and the sidelobe level increases as the code bandwidth raises. Hence, the windowing function could not suppress the sidelobe in the case of large code bandwidth, and the dynamic range decreases to $\sim 20$ dB as the number of chips goes $N_c = 1024$. On the other hand, the PLC group delay filter receiver has a proper Sinc-like target response due to recovering beat signal, and the sidelobe levels are suppressed using the window function. It is observed that this receiver provides more than $60$ dB dynamic range while using code bandwidth up to $B_c = 40$ MHz ($N_c = 1024$).

Then, we investigate the range-Doppler profiles of two signal processing methods using $N_c = 1024$ in Fig. 2. For each receiver, we apply $80$ dB Chebyshev window in the range domain before processing. For the Doppler processing, we use $N_p = 32$ number of chirp pulses, where each chirp uses a different phase-coded signal. As a consequence, there is an additional $10\log_{10}(N_p) = 15$ dB processing gain. The Doppler processing parts are the same for both receivers, and we apply $60$ dB Chebyshev window in the Doppler domain before taking FFT in the slow-time. We observe that both processing methods properly detect the moving target at $10$ m/s. However, the filter bank approach suffers from increased sidelobe levels. Moreover, it is important to note that the PLC group delay filter receiver has a lower computational complexity $\mathcal{O}(N\log_2(N))$ than the filter bank approach $\mathcal{O}(N^2)$.

### 4.2. Communication Performance

For the numerical simulations, we assume the received signal (2) is obtained along with the complex white Gaussian noise with a power spectral density $N_0$, and we define SNR $= {\alpha_0}^2/N_0$. The received signal is mixed with the reference signal, as explained in Section 3. Then, the mixer output is low-pass filtered with $f_{cut} = \pm 40$ MHz and sampled with $f_s = 80$ MHz. After delay compensation, the filter bank method obtains the received communication signal as given in (16). For the PLC group delay filter receiver, we apply the group delay filter to the received communication signal. Then, we apply the Viterbi Algorithm to reconstruct the communication data. First, we investigate the distortion effect on the received code due to the group delay filter. To focus on the impact, we consider a noise-free case and demonstrate the spectrogram

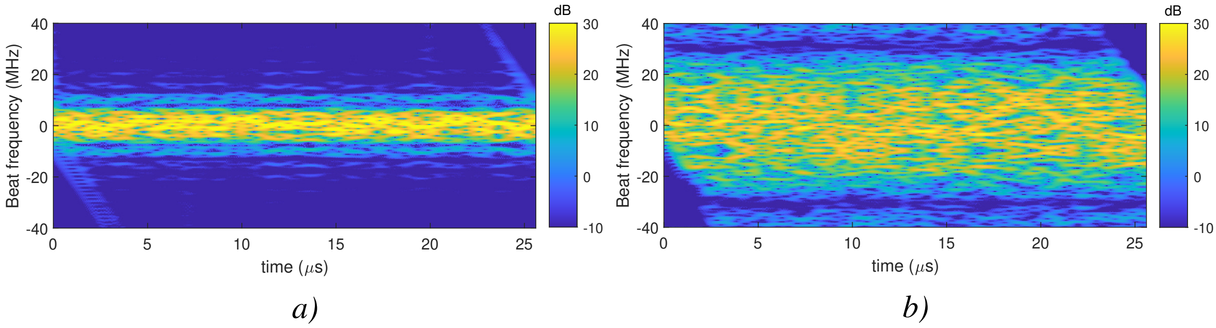


Figure 3: Spectrogram of the communication signal after PLC and group delay filter: a) $N_c = 256$ b) $N_c = 1024$

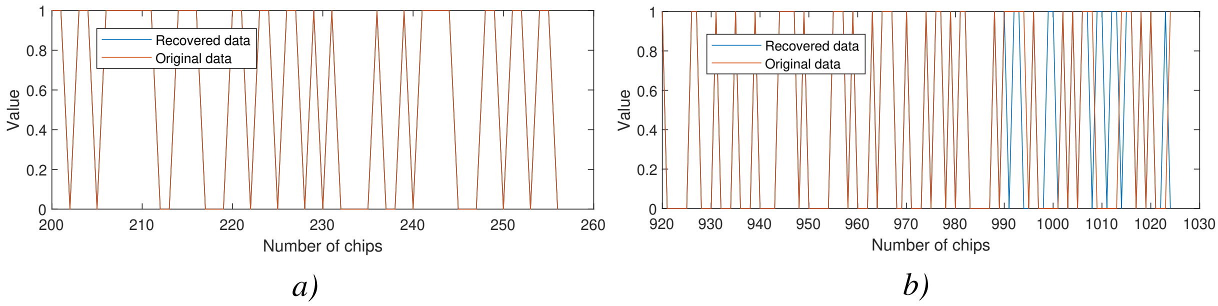


Figure 4: Recovered data with a different code bandwidth after using PLC group delay receiver: a) $N_c = 256$ b) $N_c = 1024$

of the communication signal after PLC and group delay filter in Fig. 3. It can be seen that the group delay filter applies a non-linear frequency shift and distorts the received communication signal. Such a distortion becomes cruel when the code bandwidth increases as it is affected more by the non-linear shifts (Fig. 3 b). To examine this issue, we illustrate the recovered data with a different code bandwidth for the noise-free case in Fig. 4. It can be observed that the communication data is fully recovered with $N_c = 256$ case. However, the code with $N_c = 1024$ chips is not recovered properly due to the severe distortion effect on the code, the end of the recovered communication data is obtained differently than the original data (Fig. 4 b). To avoid such a problem, the guarding cells need to be placed on the transmitted communication signal. The application of proper guarding cells to protect the received communication data from this distortion effect is a subject to be considered in future. To highlight the degradation in the communication performance, we compare the bit error rate versus SNR for both processing methods in Fig. 5. We set the noise power $N_0$ relative to the absolute of $\alpha_0$ and change SNR in the interval $SNR \in [-25, 25]$ dB. For a given SNR, we perform $100$ trials with different code sequences and count the number of errors. Note that both receivers use the same code sequence during each iteration for a fair comparison. Then for a given SNR, we calculate the bit error rate as the ratio between the total number of errors and the total number of chips. As shown in Fig. 5, the bit error rate is comparable up to $N_c = 256$ in the low SNR cases for both processing methods. Thereafter, the PLC group delay filter provides a notably higher bit error rate. In particular, the bit error rate raises up to $\sim 10^{-2}$ as the number of chips goes $N_c = 1024$ in $5$ dB SNR case. It can be seen that the bit error rate of the PLC group delay filter receiver remains stable for the codes with more than $N_c = 256$ symbols, although SNR increases.

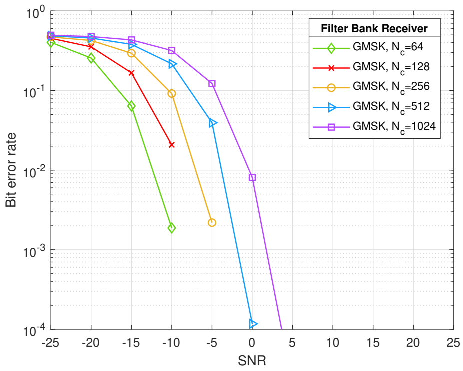


*a)*

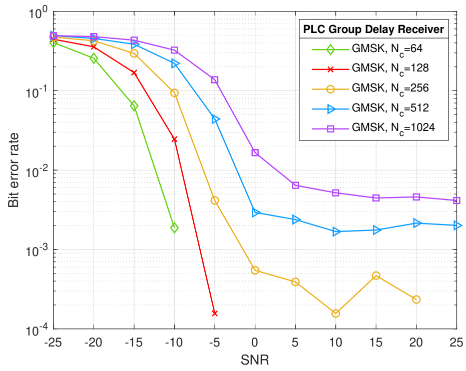


*b)*

Figure 5: Communication performance comparison: Bit error rate versus SNR a) Filter bank receiver b) PLC group delay filter receiver

# 5. Conclusion

The performance of phase-coded FMCW radars with dechirping receivers for joint sensing and communication applications is studied. We compared the communication and sensing performance of the PC-FMCW waveform processed with the phase lag compensated group delay filter and filter bank receivers. The phase lag compensated group delay filter receiver aims to obtain a beat signal similar to conventional FMCW radar by decoding the communication signal before signal processing. Thus, it can utilize techniques previously developed for the FMCW radar, such as windowing functions to reduce sidelobe levels. Consequently, the phase lag compensated group delay receiver provides better sensing performance. Moreover, the phase lag compensated group delay receiver uses FFT instead of matrix multiplication, and therefore it requires less computational complexity than the filter bank method. However, these advantages come with the price of distorting the communication signal. The reason for distortion is that the phase lag compensated group delay filter receiver applies a non-linear shift to the communication signal, which results in losing some part of the communication signal during data recovery. Thus, the phase lag compensated group delay receiver provides worse communication performance than the filter bank approach. It is shown that bit error rate degradation increases with code bandwidth.

# References


[1] C. Aydogdu, M. F. Keskin, G. K. Carvajal, O. Eriksson, H. Hellsten, H. Herbertsson, E. Nilsson, M. Rydstrom, K. Vanas, and H. Wymeersch, "Radar interference mitigation for automated driving: Exploring proactive strategies," *IEEE Signal Processing Magazine*, vol. 37, no. 4, pp. 72–84, 2020.

[2] U. Kumbul, F. Uysal, C. S. Vaucher, and A. Yarovoy, "Automotive radar interference study for different radar waveform types," *IET Radar, Sonar & Navigation*, vol. 16, no. 3, pp. 564–577, 2022. [Online]. Available: https://ietresearch.onlinelibrary.wiley.com/doi/abs/10.1049/rsn2.12203

[3] H. Griffiths, L. Cohen, S. Watts, E. Mokole, C. Baker, M. Wicks, and S. Blunt, "Radar spectrum engineering and management: Technical and regulatory issues," *Proceedings of the IEEE*, vol. 103,

no. 1, pp. 85–102, 2015.

[4] K. V. Mishra, M. R. Bhavani Shankar, V. Koivunen, B. Ottersten, and S. A. Vorobyov, "Toward millimeter-wave joint radar communications: A signal processing perspective," *IEEE Signal Processing Magazine*, vol. 36, no. 5, pp. 100–114, 2019.

[5] F. Liu, C. Masouros, A. Petropulu, H. Griffiths, and L. Hanzo, "Joint radar and communication design: Applications, state-of-the-art, and the road ahead," *IEEE Transactions on Communications*, vol. 68, pp. 3834–3862, 2020.

[6] C. Aydogdu, M. F. Keskin, N. Garcia, H. Wymeersch, and D. W. Bliss, "RadChat: Spectrum sharing for automotive radar interference mitigation," *IEEE Transactions on Intelligent Transportation Systems*, vol. 22, no. 1, pp. 416–429, 2021.

[7] M. F. Keskin, R. F. Tigrek, C. Aydogdu, F. Lampel, H. Wymeersch, A. Alvarado, and F. M. J. Willems, "Peak sidelobe level based waveform optimization for ofdm joint radar-communications," in *2020 17th European Radar Conference (EuRAD)*, 2021, pp. 1–4.

[8] S. A. Hassani, V. Lampu, K. Parashar, L. Anttila, A. Bourdoux, B. v. Liempd, M. Valkama, F. Horlin, and S. Pollin, "In-band full-duplex radar-communication system," *IEEE Systems Journal*, vol. 15, no. 1, pp. 1086–1097, 2021.

[9] C. Sahin, J. Jakabosky, P. M. McCormick, J. G. Metcalf, and S. D. Blunt, "A novel approach for embedding communication symbols into physical radar waveforms," in *2017 IEEE Radar Conference (RadarConf)*, 2017, pp. 1498–1503.

[10] F. Lampel, F. Uysal, F. Tigrek, S. Orru, A. Alvarado, F. Willems, and A. Yarovoy, "System level synchronization of phase-coded fmcw automotive radars for radcom," in *2020 14th European Conference on Antennas and Propagation (EuCAP)*, 2020, pp. 1–5.

[11] M. Bekar, C. J. Baker, E. G. Hoare, and M. Gashinova, "Joint mimo radar and communication system using a psk-lfm waveform with tdm and cdm approaches," *IEEE Sensors Journal*, vol. 21, no. 5, pp. 6115–6124, 2021.

[12] U. Kumbul, N. Petrov, F. van der Zwan, C. S. Vaucher, and A. Yarovoy, "Experimental investigation of phase coded fmcw for sensing and communications," in *2021 15th European Conference on Antennas and Propagation (EuCAP)*, 2021, pp. 1–5.

[13] U. Kumbul, N. Petrov, C. S. Vaucher, and A. Yarovoy, "Sensing performance of different codes for phase-coded fmcw radars," in *2022 19th European Radar Conference (EuRAD)*, 2022, pp. 1–4.

[14] P. M. McCormick, C. Sahin, S. D. Blunt, and J. G. Metcalf, "FMCW implementation of phase-attached radar-communications (PARC)," in *2019 IEEE Radar Conference (RadarConf)*, 2019, pp. 1–6.

[15] F. Lampel, R. F. Tigrek, A. Alvarado, and F. M. J. Willems, "A performance enhancement technique for a joint fmcw radcom system," in *2019 16th European Radar Conference (EuRAD)*, 2019, pp. 169–172.

[16] U. Kumbul, N. Petrov, C. S. Vaucher, and A. Yarovoy, "Receiver structures for phase modulated fmcw radars," in *2022 16th European Conference on Antennas and Propagation (EuCAP)*, 2022, pp. 1–5.

[17] U. Kumbul, N. Petrov, C. S. Vaucher, and A. Yarovoy, "Smoothed phase-coded FMCW: Waveform properties and transceiver architecture," *IEEE Transactions on Aerospace and Electronic Systems*, early access, Sep. 2022. doi: 10.1109/TAES.2022.3206173.

[18] M. K. Simon, *Bandwidth-Efficient Digital Modulation with Application to Deep Space Communications*. New Jersey: John Wiley & Sons, Inc., 2003.